PROCEEDINGS A

rspa.royalsocietypublishing.org

Research

Cite this article: Zohdi TI. 2018 An upper bound on the particle-laden dependency of shear stresses at solid–fluid interfaces. *Proc. R. Soc. A* **474**: 20170332.
http://dx.doi.org/10.1098/rspa.2017.0332

Received: 10 May 2017
Accepted: 20 February 2018

Subject Areas:
Mechanical engineering

Keywords:
particle-laden fluids, solid–fluid interface, shear stresses

Author for correspondence:
T. I. Zohdi
e-mail: zohdi@berkeley.edu

An upper bound on the particle-laden dependency of shear stresses at solid–fluid interfaces

T. I. Zohdi

Department of Mechanical Engineering, 6117 Etcheverry Hall, University of California, Berkeley, CA 94720-1740, USA

TIZ, 0000-0002-0844-3573

In modern advanced manufacturing processes, such as three-dimensional printing of electronics, fine-scale particles are added to a base fluid yielding a modified fluid. For example, in three-dimensional printing, particle-functionalized inks are created by adding particles to freely flowing solvents forming a mixture, which is then deposited onto a surface, which upon curing yields desirable solid properties, such as thermal conductivity, electrical permittivity and magnetic permeability. However, wear at solid–fluid interfaces within the machinery walls that deliver such particle-laden fluids is typically attributed to the fluid-induced shear stresses, which increase with the volume fraction of added particles. The objective of this work is to develop a rigorous *strict upper bound* for the tolerable volume fraction of particles that can be added, while remaining below a given stress threshold at a fluid–solid interface. To illustrate the bound's utility, the expression is applied to a series of classical flow regimes.

1. Introduction

Within the last decade, several industrialized countries have stressed the importance of advanced manufacturing to their economies. Many of these plans have highlighted the development of additive manufacturing techniques, such as three-dimensional printing. Specialized materials and the precise design of their properties are key factors in the processes. Specifically, particle-functionalized materials play a central role in this field, for example modifying inks by adding particles to freely flowing

THE ROYAL SOCIETY PUBLISHING

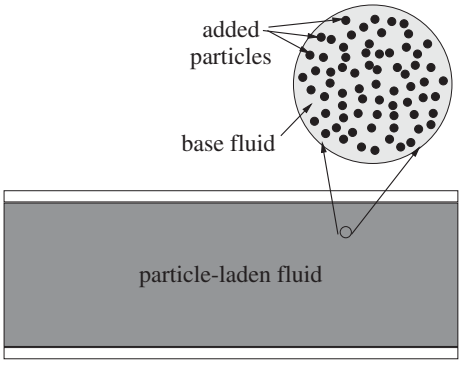

Figure 1. A particle-laden fluid.

solvents forming a mixture (figure 1), which is then deposited onto a surface and subsequently cures. For example, functionalized ink materials (primarily for printed electronics) are comprised of particles in a solvent/lubricant. Oftentimes, these inks are used to lay down electric circuit lines or to have some other specific electromagnetic function on a surface. For example, applications include optical coatings and photonics [1], MEMS applications [2–4] and biomedical devices [5]. In terms of processing techniques, we refer the reader to Sirringhaus *et al.* [6], Wang *et al.* [7], Huang *et al.* [8], Choi *et al.* [9–12], Demko *et al.* [13,14] and Zohdi [15] for details.[1] We remark that functionalized, particle-laden inks are now very important in bioprinting applications, nano-structure laden materials that can be used for sensing, as well as bioinspired, tough composites for purely mechanical applications.

In the majority of the mentioned cases, the associated manufacturing processes employ flow regimes that are laminar and Newtonian. Wear at solid–fluid interfaces within the machinery walls that carry such particle-laden fluids is attributed to the fluid-induced shear stresses, which increase with the volume fraction of added particles. The objective of this work is to develop a strict upper bound in the tolerable volume fraction of particles that can be added while remaining below a given stress threshold at a fluid–solid interface.

(a) Strict lower bounds on the effective viscosity

One of the first models for the effective viscosity of such fluids was developed in 1906 by Einstein [18], but is only accurate at extremely low volume fractions of particles ($\ll$1%). It reads as

$$\mu^* = \mu_f(1 + 2.5\nu_p), \tag{1.1}$$

where μ^* is the effective viscosity, μ_f is the viscosity of the fluid and ν_p is the volume fraction of particles. A more accurate approximation, *in fact a strict, rigorous, lower bound* (accurate up to approximately $\nu_p \approx 15\%$, which is sufficient for many applications of interest) can be derived from the well-known Hashin & Shtrikman [19–21] bounds in solid mechanics, which is discussed next.

The literature on methods to estimate the overall effective solid properties of heterogeneous materials dates back at least to Maxwell [22,23] and Lord Rayleigh [24], with a notable contribution being the Hashin–Shtrikman bounds [19–21]. Specifically, for linearized elasticity applications, for isotropic materials with isotropic effective (mechanical) responses, the

[1]For reviews of optical coatings and photonics, see Nakanishi *et al.* [1] and Maier & Atwater [16], for catalysts, see Haruta [17] and for MEMS applications, see Fuller *et al.* [2].

Hashin–Shtrikman bounds (for a two-phase material) are as follows for the effective bulk modulus (κ^*)

$$\kappa^{*,-} \overset{\text{def}}{=} \kappa_1 + \frac{\nu_2}{1/(\kappa_2-\kappa_1)+3(1-\nu_2)/(3\kappa_1+4\mu_1)} \leq \kappa^* \leq \kappa_2 + \frac{1-\nu_2}{1/(\kappa_1-\kappa_2)+3\nu_2/(3\kappa_2+4\mu_2)} \overset{\text{def}}{=} \kappa^{*,+} \tag{1.2}$$

and for the effective shear modulus (G^*)

$$G^{*,-} \overset{\text{def}}{=} G_1 + \frac{\nu_2}{1/(G_2-G_1)+6(1-\nu_2)(\kappa_1+2G_1)/5G_1(3\kappa_1+4G_1)} \leq G^* \leq G_2 + \frac{(1-\nu_2)}{1/(G_1-G_2)+6\nu_2(\kappa_2+2G_2)/5G_2(3\kappa_2+4G_2)} \overset{\text{def}}{=} G^{*,+}, \tag{1.3}$$

where κ_1 (usually the matrix material) and κ_2 (usually the particulate material) are the bulk moduli, and G_1 and G_2 are the shear moduli of the respective phases ($\kappa_2 \geq \kappa_1$ and $G_2 \geq G_1$), and where ν_2 is the second phase volume fraction. Such bounds are the tightest possible on isotropic effective responses, with isotropic two-phase microstructures, where only the volume fractions and phase contrasts of the constituents are known (see [21] for a discussion on the optimality of such bounds). Note that no geometric or statistical information is required for the bounds. For an authoritative review of the general theory of random heterogeneous media see Torquato [25]. For more mathematical homogenization aspects, see Jikov *et al.* [26], while for solid-mechanics inclined accounts of the subject see Hashin [21], Mura [27] or Markov [28]. To represent rigid particles in an incompressible fluid, one can take the limit of the particle phase becoming rigid, i.e. the bulk and shear moduli tending towards infinity, $\kappa_2 = \kappa_\mathrm{p} \to \infty$ and $G_2 = \mu_\mathrm{p} \to \infty$, signifying that the particles are much stiffer than the interstitial fluid (assigning the elastic shear modulus G_1 to the fluid viscosity μ_f), while simultaneously specifying that the interstitial fluid is incompressible, i.e. $\kappa_1/G_1 = \kappa_\mathrm{f}/\mu_\mathrm{f} \to \infty$ (with G_1 being finite). This yields, for the lower Hashin–Shtrikman bound[2]

$$\mu^{*,-} = \mu_\mathrm{f}\left(1 + 2.5\frac{\nu_p}{1-\nu_\mathrm{p}}\right). \tag{1.4}$$

Equation (1.4) represents the tightest known lower bound on the effective viscosity of a two-phase material comprised of rigid particles in a surrounding incompressible fluid. We refer the reader to Sevostianov & Kachanov [29] and Kachanov & Abedian [30] for in depth reviews. The bound recaptures the Einstein result in the $\nu_\mathrm{p} \to 0$ limit, but is a rigorous lower bound at significant ν_p. This rigorous lower bound is extremely accurate up to approximately 15% volume fraction. These bounds have been tested in the numerical analysis literature repeatedly, for example, against direct finite-element calculations found in Zohdi & Wriggers [31], Ghosh [32] and Ghosh & Dimiduk [33]. This is discussed further later in the paper.

Remark. It is critical to emphasize that we assume that not only the base fluid is Newtonian, but also that particle-base fluid combination behaves in Newtonian manner.

(b) Subsequent strict upper bounds on the tolerable particle volume fraction

Consider the following Newtonian relation:

$$\boldsymbol{\tau} = 2\mu^* \boldsymbol{D}(\boldsymbol{v}), \tag{1.5}$$

where $\boldsymbol{\tau}$ is the viscous stress, μ^* is the effective viscosity and $\boldsymbol{D} = \frac{1}{2}(\nabla \boldsymbol{v} + (\nabla \boldsymbol{v})^\mathrm{T})$. There is a large number of classical velocity fields (examples will be given shortly) which are independent of the

[2]The upper bound yields no valuable information; i.e. $\mu^{*,+} \to \infty$.

viscosity of the fluid (when the volumetric flow rate is controlled)

$$\boldsymbol{v} \neq \boldsymbol{v}(\mu^*). \tag{1.6}$$

Thus, if we employ a lower bound on μ^*, we obtain

$$\mu^{*,-}\|2\boldsymbol{D}(\boldsymbol{v})\| \leq \mu^*\|2\boldsymbol{D}(\boldsymbol{v})\| = \|\boldsymbol{\tau}\| = \tau^{\text{crit}}, \tag{1.7}$$

where τ^{crit} is a preset critical shear stress threshold which one does not wish to exceed. Thus,

$$\mu^{*,-} \leq \frac{\tau^{\text{crit}}}{\|2\boldsymbol{D}(\boldsymbol{v})\|}, \tag{1.8}$$

or explicitly

$$\mu^{*,-} = \mu_f\left(1 + 2.5\frac{\nu_{\text{p}}}{1-\nu_{\text{p}}}\right) \leq \frac{\tau^{\text{crit}}}{\|2\boldsymbol{D}(\boldsymbol{v})\|}, \tag{1.9}$$

or compactly

$$\nu_{\text{p}} \leq \frac{\tau^{\text{crit}} - \mu_{\text{f}}\|2\boldsymbol{D}(\boldsymbol{v})\|}{\tau^{\text{crit}} + (3/2)\mu_{\text{f}}\|2\boldsymbol{D}(\boldsymbol{v})\|}. \tag{1.10}$$

This provides a strict upper bound on the volume fraction of particles that can be added while respecting a critical shear stress. To illustrate the use of this expression, three classical examples are considered:[3]

— flow through two infinite stationary plates (channel/planar Poiseuille flow),
— flow through two infinite plates with additional motion of one plate (Couette flow) and
— flow through a pipe of radius R.

2. Application: flow through two infinite stationary plates (channel/Poiseuille flow)

Referring to figure 2, assuming fully developed, steady, Newtonian flow, *with the control variable being the constant volumetric flow rate* $Q(t) = Q_o$, between two very wide (width $= w$) plates separated by a distance a, the classical solution can be written as

$$v(y) = \frac{6Q_o}{aw}\left(\frac{y}{a} - \left(\frac{y}{a}\right)^2\right). \tag{2.1}$$

The shear stress becomes

$$\tau = \mu^*\frac{\partial v(y)}{\partial y} = \mu^*\left(\frac{6Q_o}{aw}\left(\frac{1}{a} - \frac{2y}{a^2}\right)\right). \tag{2.2}$$

At the walls, $y = a$ and $y = 0$

$$\left|\frac{\partial v(y)}{\partial y}\right| = \frac{6Q_o}{a^2 w}. \tag{2.3}$$

Now using equation (1.10) (where $\|2\boldsymbol{D}(\boldsymbol{v})\|$ is replaced by $|\partial v/\partial y|$) yields

$$\nu_{\text{p}} \leq \frac{\tau^{\text{crit}} - \mu_{\text{f}}(6Q_o/a^2 w)}{\tau^{\text{crit}} + \mu_{\text{f}}(9Q_o/a^2 w)}. \tag{2.4}$$

3. Application: flow through two infinite plates with additional motion of one plate (Couette flow)

Referring to figure 3, assuming fully developed, steady, Newtonian flow, with *constant volumetric flow rate* $Q(t) = Q_o$, between two very wide (width $= w$) plates separated by a distance a, with the

[3]We remark that such an expression can find uses in biological flow regimes where wall shear stress is attributed to a variety of secondary effects associated with atherosclerosis [34].

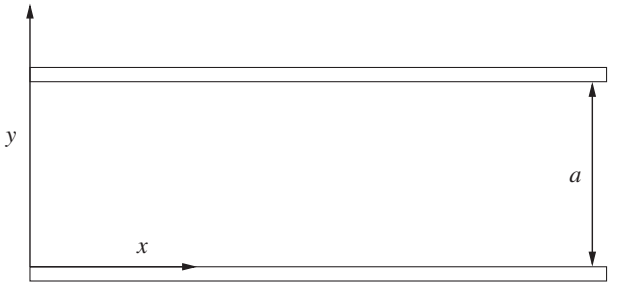

Figure 2. Flow through two very wide plates.

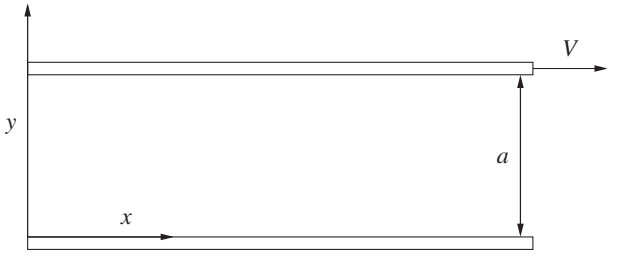

Figure 3. Flow through two very wide plates, with the top plate in motion.

top plate moving with a horizontal velocity of $\mathcal{V}$, the classical solution can be written as

$$v(y) = \frac{\mathcal{V}}{a}y - 6\left(\frac{\mathcal{V}}{2} - \frac{Q_o}{aw}\right)\left(\frac{y}{a} - \left(\frac{y}{a}\right)^2\right). \tag{3.1}$$

The shear stress becomes

$$\tau = \mu^* \frac{\partial v(y)}{\partial y} = \mu^*\left(\frac{\mathcal{V}}{a} - 6\left(\frac{\mathcal{V}}{2} - \frac{Q_o}{aw}\right)\left(\frac{1}{a} - \frac{2y}{a^2}\right)\right). \tag{3.2}$$

At the walls, $y = a$

$$\left|\frac{\partial v(y)}{\partial y}\right| = \left|\frac{\mathcal{V}}{a} + 6\left(\frac{\mathcal{V}}{2a} - \frac{Q_o}{a^2 w}\right)\right| \tag{3.3}$$

and $y = 0$

$$\left|\frac{\partial v(y)}{\partial y}\right| = \left|\frac{\mathcal{V}}{a} - 6\left(\frac{\mathcal{V}}{2a} - \frac{Q_o}{a^2 w}\right)\right|. \tag{3.4}$$

Now using equation (1.10) (where $\|2\boldsymbol{D}(\boldsymbol{v})\|$ is replaced by $|\partial v/\partial y|$) yields, for $y = a$,

$$\nu_{\mathrm{p}} \leq \frac{\tau^{\mathrm{crit}} - \mu_{\mathrm{f}}|\mathcal{V}/a + 6(\mathcal{V}/2a - Q_o/a^2 w)|}{\tau^{\mathrm{crit}} + (3/2)\mu_{\mathrm{f}}|\mathcal{V}/a + 6(\mathcal{V}/2a - Q_o/a^2 w)|}, \tag{3.5}$$

while for $y = 0$,

$$\nu_{\mathrm{p}} \leq \frac{\tau^{\mathrm{crit}} - \mu_{\mathrm{f}}|\mathcal{V}/a - 6(\mathcal{V}/2a - Q_o/a^2 w)|}{\tau^{\mathrm{crit}} + (3/2)\mu_{\mathrm{f}}|\mathcal{V}/a - 6(\mathcal{V}/2a - Q_o/a^2 w)|}. \tag{3.6}$$

(a) Special case: flow between two concentric cylinders

A special case of the previous example is the flow between two concentric cylinders (with a gap of a), where the interior cylinder is rotating with angular velocity ω and the outer cylinder being stationary (figure 4). Assuming steady flow and no angular dependence of the solution (angular

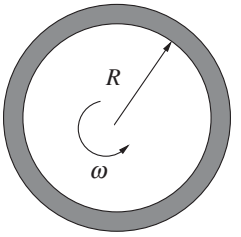

Figure 4. Flow between two concentric cylinders.

symmetry), the solution collapses to simply

$$v(y) = \frac{\mathcal{V}}{a} y, \tag{3.7}$$

where $\mathcal{V} = R\omega$, where R is the radius of the inner cylinder and ω is its angular velocity. The shear stress becomes

$$\tau = \mu^* \frac{\partial v(y)}{\partial y} = \mu^* \frac{\mathcal{V}}{a}. \tag{3.8}$$

At the walls

$$\left| \frac{\partial v(y)}{\partial y} \right| = \left| \frac{\mathcal{V}}{a} \right|. \tag{3.9}$$

Now using equation (1.10) (where $\|2\boldsymbol{D}(\boldsymbol{v})\|$ is replaced by $|\partial v/\partial y|$) yields

$$\nu_{\mathrm{p}} \leq \frac{\tau^{\mathrm{crit}} - \mu_{\mathrm{f}} |\mathcal{V}/a|}{\tau^{\mathrm{crit}} + (3/2)\mu_{\mathrm{f}} |\mathcal{V}/a|}. \tag{3.10}$$

4. Flow through a pipe of radius R

Referring to figure 5, we consider a pipe with radius R and a circular cross-sectional area of $A = \pi R^2$. Assuming fully developed, steady, Newtonian flow, with constant volumetric flow rate $Q(t) = Q_o$, one obtains

$$v(r) = \frac{2Q_o}{A} \left(1 - \left(\frac{r}{R} \right)^2 \right). \tag{4.1}$$

The stress becomes

$$\tau(r) = \mu^* \frac{\partial v(r)}{\partial r} = -\frac{4\mu^* Q_o r}{\pi R^4}. \tag{4.2}$$

Using equation (1.10) yields (where $\|2\boldsymbol{D}(\boldsymbol{v})\|$ is replaced by $|\partial v/\partial r|$), for $r = R$,

$$\nu_{\mathrm{p}} \leq \frac{\tau^{\mathrm{crit}} - \mu_{\mathrm{f}} (4Q_o/\pi R^3)}{\tau^{\mathrm{crit}} + \mu_{\mathrm{f}} (6Q_o/\pi R^3)}. \tag{4.3}$$

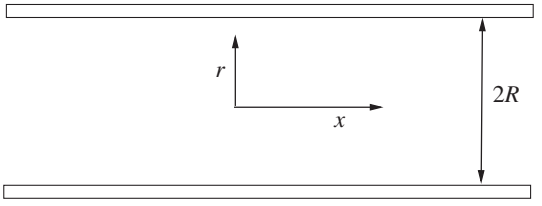

Figure 5. Flow through a pipe.

5. Comparative analysis with a commonly used estimate

A widely used effective viscosity estimate is that of Oliver & Ward [35] which, *although not a rigorous bound*, is much better agreement with experimental data up to $\nu_p = 0.30$ (see [29,30] for extensive reviews). It reads as

$$\mu^* \approx \mu^{*e} = \frac{\mu_f}{1 - 2.5\nu_p}. \tag{5.1}$$

Repeating the analysis with this expression (equation (5.1) instead of (1.4)), we start with

$$\boldsymbol{\tau} = 2\mu^* \boldsymbol{D}(\boldsymbol{v}) \Rightarrow \mu^* \|2\boldsymbol{D}(\boldsymbol{v})\| \leq \mu^* \|2\boldsymbol{D}(\boldsymbol{v})\| = \|\boldsymbol{\tau}\| = \tau^{\text{crit}} \tag{5.2}$$

and inserting

$$\mu^{*e} = \frac{\mu_f}{1 - 2.5\nu_p} \approx \frac{\tau^{\text{crit}}}{\|2\boldsymbol{D}(\boldsymbol{v})\|} \tag{5.3}$$

yields

$$\nu_p^e \approx \frac{2}{5}\left(1 - \frac{\mu_f \|2\boldsymbol{D}(\boldsymbol{v})\|}{\tau^{\text{crit}}}\right). \tag{5.4}$$

This provides an estimate on the volume fraction of particles that can be added, while respecting a critical shear stress limit. As the basis of this expression is the effective property estimate, which is accurate for up to $\nu_p = 0.30$ [29,30], we can assume a subsequent high level of fidelity for the volume fraction estimates. To compare the estimate to the rigorous lower bound we define two predicted effective viscosities, one from the bound ($\stackrel{\text{def}}{=} \mu^{*-}$) and the other from the Oliver & Ward [35] estimate ($\stackrel{\text{def}}{=} \mu^{*e}$) and take their ratio

$$\Phi \stackrel{\text{def}}{=} \frac{\mu^{*-}}{\mu^{*e}} = \frac{\mu_f(1 + 2.5(\nu_p/(1-\nu_p)))}{\mu_f/(1 - 2.5\nu_p)} = \frac{1 - \nu_p - 3.75\nu_p^2}{1 - \nu_p} \leq 1, \tag{5.5}$$

which is always less than unity for finite ν_p. Numerical results are shown in table 1. The agreement is reasonable up to about $\nu_p \approx 15\%$. The subsequent ratio of resulting predicted tolerable volume fractions of the bound ($\stackrel{\text{def}}{=} \nu_p^-$) and the Oliver & Ward [35] estimate ($\stackrel{\text{def}}{=} \nu_p^e$) is

$$\Gamma \stackrel{\text{def}}{=} \frac{\nu_p^-}{\nu_p^e} = \frac{(\tau^{\text{crit}} - \mu_f\|2\boldsymbol{D}(\boldsymbol{v})\|)/(\tau^{\text{crit}} + (3/2)\mu_f\|2\boldsymbol{D}(\boldsymbol{v})\|)}{(2/5)(1 - \mu_f\|2\boldsymbol{D}(\boldsymbol{v})\|/\tau^{\text{crit}})} = \frac{5}{2 + 3(\mu_f\|2\boldsymbol{D}(\boldsymbol{v})\|/\tau^{\text{crit}})} \geq 1, \tag{5.6}$$

which is always greater than unity, since $\tau^{\text{crit}} \geq \mu_f\|2\boldsymbol{D}(\boldsymbol{v})\|$. Finally, in order to illustrate the use of this estimate, again consider the three classical examples from before:

— flow through two infinite stationary plates (channel/planar Poiseuille flow), where $\|2\boldsymbol{D}(\boldsymbol{v})\|$ is replaced by $|\partial v(y)/\partial y| = 6Q_o/a^2 w$, yielding

$$\nu_p^e \approx \frac{2}{5}\left(1 - \frac{\mu_f\|2\boldsymbol{D}(\boldsymbol{v})\|}{\tau^{\text{crit}}}\right) = \frac{2}{5}\left(1 - \frac{6\mu_f Q_o}{a^2 w \tau^{\text{crit}}}\right). \tag{5.7}$$

Table 1. A comparison of the two predicted effective viscosities: from the bound ($\stackrel{\text{def}}{=}\mu^{*-}$) and the Oliver & Ward [35] estimate ($\stackrel{\text{def}}{=}\mu^{*e}$).

ν_{p}	Φ
0	1
0.10	0.958
0.15	0.900
0.25	0.687
0.30	0.518

— flow through two infinite plates with additional motion of one plate (Couette flow), where $\|2\boldsymbol{D}(\boldsymbol{v})\|$ is replaced by $|\partial v(y)/\partial y| = |\mathcal{V}/a|$, yielding

$$\nu_{\text{p}}^{e} \approx \frac{2}{5}\left(1 - \frac{\mu_{\text{f}}\|2\boldsymbol{D}(\boldsymbol{v})\|}{\tau^{\text{crit}}}\right) = \frac{2}{5}\left(1 - \left|\frac{\mu_{\text{f}}\mathcal{V}}{a\tau^{\text{crit}}}\right|\right). \tag{5.8}$$

— flow through a pipe of radius R, where $\|2\boldsymbol{D}(\boldsymbol{v})\|$ is replaced by $|\partial v/\partial r| = 4Q_o r/\pi R^4$, yielding, for $r = R$,

$$\nu_{\text{p}}^{e} \approx \frac{2}{5}\left(1 - \frac{\mu_{\text{f}}\|2\boldsymbol{D}(\boldsymbol{v})\|}{\tau^{\text{crit}}}\right) = \frac{2}{5}\left(1 - \frac{4\mu_{\text{f}}Q_o}{\pi R^3\tau^{\text{crit}}}\right). \tag{5.9}$$

The preceding analysis simply provides a comparative example with one such effective viscosity estimate, and could be repeated for others found in the literature. We emphasize that the objective was to formulate a conservative upper-bound that can be used to safely design systems involving particle-laden flows.

6. Conclusion

In this work, lower bounds from the field of particle-laden solid mechanics were adopted to generate a lower bound on the effective viscosity of a Newtonian base fluid with embedded rigid particles. This expression was then in turn used to generate a strict upper bound in the tolerable volume fraction of particles that can be added, while respecting a critical stress threshold at a fluid–solid interface. The derived expression, equation (1.10), is simple to use, and was applied to some classical problems, for illustration purposes. The expression should be quite useful in the analysis of fluid-induced shear stresses in advanced manufacturing processes [36], where functionalizing particles are added to a base fluid, with viscosity μ_{f}, to produce a type a new fluid, with effective viscosity, μ^*. In addition to the industrial examples that were discussed in the Introduction, we further mention that electromagnetic fluids are typically functionalized by embedding charged or electromagnetically sensitive particles in a neutral fluid. Such fluids date back, at least, to Winslow [37,38] in 1947. While the most widely used class of such fluids are electrorheological fluids, which are comprised of extremely fine suspensions of charged particles (on the order of 1–5 μ) in an electrically neutral fluid, there has been a renewed interest in this class of materials because of so-called e-inks (electrically functionalized inks) driven by printed electronics. Electrical inkjet printing is attractive due to its high throughput. This, of course, comes with increases in the Reynolds number, which in turn will lead to potentially turbulent flow. Currently, patterning with inkjet printing is limited to a resolution of around 20–50 μm with current printers [39] with higher resolution possible by adding complexity to the substrate prior to printing [7]. Electrohydrodynamic printing has also been proposed to increase the resolution beyond the limits of inkjet printing, achieving a line resolution as small as 700 nm [40]. There are a variety of related high-throughput industrial deposition techniques, and we refer the reader to the surveys of the state of the art found in Martin [41,42], as well as the extensive works of

Choi and co-workers [9–12] and Demko *et al.* [13], and the extension of equation (1.10) to those regimes is under current investigation by the author.

Data accessibility. This article has no additional data.

Competing interests. I declare I have no competing interests.

Funding. We received no funding for this study.

Acknowledgements. The author wishes to thank Dr Debanjan Mukherjee, Dr Chang-Yoon Park and Dr Erden Yildizdag for their proofreading and comments during the revision of this work.

References

1. Nakanishi H *et al.* 2009 Photoconductance and inverse photoconductance in thin films of functionalized metal nanoparticles. *Nature* **460**, 371–375. (doi:10.1038/nature08131)
2. Fuller SB, Wilhelm EJ, Jacobson JM. 2002 Ink-jet printed nanoparticle microelectromechanical systems. *J. Microelectromech. Syst.* **11**, 54–60. (doi:10.1109/84.982863)
3. Samarasinghe SR, Pastoriza-Santos I, Edirisinghe MJ, Reece MJ, Liz-Marzan LM. 2006 Printing gold nanoparticles with an electrohydrodynamic direct write device. *Gold Bull.* **39**, 48–53. (doi:10.1007/BF03215276)
4. Gamota D, Brazis P, Kalyanasundaram K, Zhang J. 2004 *Printed organic and molecular electronics*. New York, NY: Kluwer Academic Publishers.
5. Ahmad Z, Rasekh M, Edirisinghe M. 2010 Electrohydrodynamic direct writing of biomedical polymers and composites. *Macromol. Mater. Eng.* **295**, 315–319. (doi:10.1002/mame.200900396)
6. Sirringhaus H, Kawase T, Friend RH, Shimoda T, Inbasekaran M, Wu W, Woo EP. 2000 High-resolution inkjet printing of all-polymer transistor circuits. *Science* **290**, 2123–2126. (doi:10.1126/science.290.5499.2123)
7. Wang JZ, Zheng ZH, Li HW, Huck WTS, Sirringhaus H. 2004 Dewetting of conducting polymer inkjet droplets on patterned surfaces. *Nat. Mater.* **3**, 171–176. (doi:10.1038/nmat1073)
8. Huang D, Liao F, Molesa S, Redinger D, Subramanian V. 2003 Plastic-compatible low-resistance printable gold nanoparticle conductors for flexible electronics. *J. Electrochem. Soc.* **150**, G412–G417. (doi:10.1149/1.1582466)
9. Choi S, Park I, Hao Z, Holman HY, Pisano AP, Zohdi TI. 2010 Ultra-fast self-assembly of micro-scale particles by open channel flow. *Langmuir* **26**, 4661–4667. (doi:10.1021/la903492w)
10. Choi S, Stassi S, Pisano AP, Zohdi TI. 2010 Coffee-ring effect-based three dimensional patterning of micro, nanoparticle assembly with a single droplet. *Langmuir* **26**, 11 690–11 698. (doi:10.1021/la101110t)
11. Choi S, Jamshidi A, Seok TJ, Zohdi TI, Wu MC, Pisano AP. 2012 Fast, High-throughput creation of size-tunable micro, nanoparticle clusters via evaporative self-assembly in picoliter-scale droplets of particle suspension. *Langmuir* **28**, 3102–3111. (doi:10.1021/la204362s)
12. Choi S, Pisano AP, Zohdi TI. 2013 An analysis of evaporative self-assembly of micro particles in printed picoliter suspension droplets. *J. Thin Solid Films* **537**, 180–189. (doi:10.1016/j.tsf.2013.04.047)
13. Demko M, Choi S, Zohdi TI, Pisano AP. 2012 High resolution patterning of nanoparticles by evaporative self-assembly enabled by in-situ creation and mechanical lift-off of a polymer template. *Appl. Phys. Lett.* **99**, 253102. (doi:10.1063/1.3671084)
14. Demko MT, Cheng JC, Pisano AP. 2010 High-resolution direct patterning of gold nanoparticles by the microfluidic molding process. *Langmuir* **2010**, 16 710–16 714. (doi:10.1021/la1022533)
15. Zohdi TI. 2012 Estimation of electrical-heating load-shares for sintering of powder mixtures. *Proc. R. Soc. A* **468**, 2174–2190. (doi:10.1098/rspa.2011.0755)
16. Maier SA, Atwater HA. 2005 Plasmonics: localization and guiding of electromagnetic energy in metal/dielectric structures. *J. Appl. Phys.* **98**, 011101. (doi:10.1063/1.1951057)
17. Haruta M. 2002 Catalysis of gold nanoparticles deposited on metal oxides. *Cattech.* **6**, 102–115. (doi:10.1023/A:1020181423055)
18. Einstein A. 1906 A new determination of molecular dimensions. *Ann. Phys.* **19**, 289–306.
19. Hashin Z, Shtrikman S. 1962 On some variational principles in anisotropic and nonhomogeneous elasticity. *J. Mech. Phys. Solids* **10**, 335–342. (doi:10.1016/0022-5096(62)90004-2)
20. Hashin Z, Shtrikman S. 1963 A variational approach to the theory of the elastic behaviour of multiphase materials. *J. Mech. Phys. Solids* **11**, 127–140. (doi:10.1016/0022-5096(63)90060-7)

21. Hashin Z. 1983 Analysis of composite materials: a survey. *ASME J. Appl. Mech.* **50**, 481–505. (doi:10.1115/1.3167081)
22. Maxwell JC. 1867 On the dynamical theory of gases. *Philos. Trans. R. Soc. Lond.* **157**, 49–88. (doi:10.1098/rstl.1867.0004)
23. Maxwell JC. 1873 *A treatise on electricity and magnetism*, 3rd edn. Oxford, UK: Clarendon Press.
24. Rayleigh JW (Lord Raleigh). 1892 On the influence of obstacles arranged in rectangular order upon properties of a medium. *Philos. Mag.* **32**, 481–491.
25. Torquato S. 2002 *Random heterogeneous materials: microstructure and macroscopic properties*. New York, NY: Springer-Verlag.
26. Jikov VV, Kozlov SM, Olenik OA. 1994 *Homogenization of differential operators and integral functionals*. Berlin, Germany: Springer-Verlag.
27. Mura T. 1993 *Micromechanics of defects in solids*, 2nd edn. Dordrecht, The Netherlands: Kluwer Academic Publishers.
28. Markov KZ. 2000 Elementary micromechanics of heterogeneous media. In *Heterogeneous media: micromechanics modeling methods and simulations* (eds KZ Markov, L Preziozi), pp. 1–162. Boston, MA: Birkhauser.
29. Sevostianov I, Kachanov M. 2012 Effective properties of heterogeneous materials: proper application of the non-interaction and the 'dilute limit' approximations. *Int. J. Eng. Sci.* **58**, 124–128. (doi:10.1016/j.ijengsci.2012.03.031)
30. Kachanov M, Abedian XX. 2015 On the isotropic and anisotropic viscosity of suspensions containing particles of diverse shapes and orientations. *Int. J. Eng. Sci.* **94**, 71–85. (doi:10.1016/j.ijengsci.2015.05.003)
31. Zohdi TI, Wriggers P. 2008 *Introduction to computational micromechanics*. Berlin, Germany: Springer-Verlag.
32. Ghosh S. 2011 *Micromechanical analysis and multi-scale modeling using the voronoi cell finite element method*. Boca Raton, FL/London, UK: CRC Press/Taylor & Francis.
33. Ghosh S, Dimiduk D. 2011 *Computational methods for microstructure-property relations*. New York, NY: Springer.
34. Zohdi TI. 2014 Mechanically-driven accumulation of microscale material at coupled solid-fluid interfaces in biological channels. *Proc. R. Soc. Interface* **11**, 20130922. (doi:10.1098/rsif.2013.0922)
35. Oliver DR, Ward SG. 1953 Relationship between relative viscosity and volume concentration of stable suspensions of spherical particles. *Nature* **171**, 396–397. (doi:10.1038/171396b0)
36. Zohdi TI. 2014 Embedded electromagnetically sensitive particle motion in functionalized fluids. *Comput. Part. Mech.* **1**, 27–45. (doi:10.1007/s40571-014-0013-8)
37. Winslow WM. 1947 Method and means for translating electrical impulses into mechanical force. U.S. Patent 2,417,850.
38. Winslow WM. 1949 Induced fibration of suspensions. *J. Appl. Phys.* **20**, 1137–1140. (doi:10.1063/1.1698285)
39. Ridley BA, Nivi B, Jacobson JM. 1999 All-inorganic field effect transistors fabricated by printing. *Science* **286**, 746–749. (doi:10.1126/science.286.5440.746)
40. Park J-U *et al.* 2007 High-resolution electrohydrodynamic jet printing. *Nat. Mater.* **6**, 782–789. (doi:10.1038/nmat1974)
41. Martin P. 2009 *Handbook of deposition technologies for films and coatings*, 3rd edn. Amsterdam, The Netherlands: Elsevier.
42. Martin P. 2011 *Introduction to surface engineering and functionally engineered materials*. Salem, MA: Scrivener.